49th AIAA Aerospace Sciences Meeting including the New Horizons Forum and Aerospace Exposition
4 - 7 January 2011, Orlando, Florida

AIAA 2011-761

Rarefied Compressible Two-Dimensional Jet Plume Impingement on a Flat Plate

Khaleel Khasawneh* Chunpei Cai† Hongli Liu‡
New Mexico State University, Las Cruces, New Mexico, 88003-8001

In this paper, we investigate rarefied jet gas flows out of a two-dimensional slit and impinges on a flat plate which is set vertically to the plume flow direction. With a relation between velocity-directions and geometry-positions, we obtain several analytical collisionless flow property distributions in front of the plate. This study further provides near-plate collisionless flow properties including density, slip velocity, temperature, pressure, shear stress and heat flux. Numerical simulation results obtained with the direct simulation Monte Carlo method validate the analytical collisionless flow solutions. In general, the comparisons between the exact analytical solutions and the numerical ones are virtually identical. Further, the analytical results, which are derived for the collisionless flow situation, are applicable for finite Knudsen number in the range $Kn \geq 1$. These analytical results can provide first order predictions for engineering applications with minor inaccuracies.

Nomenclature

D	nozzle width, m
f	velocity distribution function, $(m/s)^{-1}$
n	number density, kg/m^3
H	nozzle semi-width, $H = D/2$, m
L	distance from nozzle exit to the plate, m
S	rarefied gas speed ratio, $S = U/\sqrt{2RT}$
R	universal gas constant, $J/Kg\ K$
T	macroscopic temperature, K
u, v, w	microscopic molecular velocity, m/s
U, V	macroscopic average velocity, m/s
W	vertical plate semi-length, m
X, Y	point in the flowfield
β	$1/(2RT)$, Kg/J
$\Delta\theta$	solid angle subtended by the two slit tips and one point in the flowfield, $= \theta_2 - \theta_1$
Ω_1, Ω_2	specific velocity phase domains
ϕ	angle between the X-axis and a segment from (0, 0) to (X,Y)

*Graduate Student, Department of Mechanical and Aerospace Engineering, Email: kh16867@nmsu.edu.
†Assistant Professor, Department of Mechanical and Aerospace Engineering, AIAA Senior Member. Email: ccai@nmsu.edu.
‡Research Associate, Department of Mechanical and Aerospace Engineering, Email: liuhl@nmsu.edu.

ρ	density, Kg/m^3
τ	shear stress on the plate, $Pascal$
θ, θ_1, θ_2	geometry angles
subscript	
0	averaged flow properties at nozzle exit
1	macroscopic properties for the problem of plume expanding into vacuum, without the plate
2	macroscopic properties for the plume impingement problem, with the plate

I. Introduction

Jet impingement flows can be found in cooling of hot metal, such as a turbine blade, plastic, glass sheets, electronics, drying paper, fabric, and other applications. Rarefied jet flows impinging on a flat plate have many important applications as well. Several examples include: for a thin film deposition process inside a vacuum chamber, the high speed carrier gas carries metal powder and impinges on a flat plate;[1] rocket plume impinges on spacecraft solar panels.[2]

Among those examples, we are interested in the flowfield and the properties on the plate or ground. Especially, the pressure and shear stress distributions on the plate are helpful for some applications; for examples 1). computing the drag force on solar panel surfaces; 2). determining the lunar ground breaking up position and the beginning position of sand lifting up.

This paper presents some results on a highly rarefied two-dimensional jet plume flow impinging on a flat plate. In the past, the related work may classify into two categories. The first category is on free collisionless plume flows, which is the foundation for highly rarefied jet impingement flow problem; the second category is on rarefied plume jet impingement on a flat plate.

For the first problem, usually a rarefied plume jet is modeled by assuming free molecular flows with a nonzero, uniform average exit velocity, U_0. As pointed out by Woronowicz,[3] for high speed plume flows, even the number density at the exit can be high, the relative velocity is small, as such, intermolecular collisions happen rarely. Liepmann[4] reported the efflux of gases through circular apertures, which is an example of a transition from a gasdynamics to a gaskinetic regime; Narasimha[5] obtained the exact solutions of density and velocity distributions for a free molecular effusion flow; Brook[6] reported the density field of free molecular flow from an annulus to study the gas leakage effect from a spacecraft hatch. Recently, Lilly *et al* reported their work on measurement and computation of mass flow and momentum flux through short tubes in rarefied gas.[7] For the case of free molecular flows with a nonzero average velocity, usually the problems are complicated.[8] Two previous studies,[9,10] provided several detailed macroscopic solutions of collisionless plume flows; and they serve as the foundation for the rarefied plume jet impingement problem. The report by Weaver and Wysong[11] et al provides a comprehensive review of recent studies on plume impingement flows.

For the second category, there are some numerical and experimental results as well. For example, Bradshaw[12] reported measurements of velocity magnitude and direction, static pressure and skin friction for the problem of a circular air jet impinging normally on a flat surface. Sathian[13] reported a measurement of shear stress due to impingement of low-density free jets on a flat plate. Maddox[14] reported a computation method to determine the drag and heat flux by under expanded plumes to adjacent surfaces. Kannenberg and Boyd[15] proposed some results of plume impingement on a plate surface with a hyperthermal flow limit assumption.

For a lunar or Martian landing mission with a retro-rocket, the determination of the interactions among rarefied rocket plume, crater and dust is one of the most challenging tasks.[16] Due to the special environment, to perform experimental study with accurate parameters is almost impossible, and we have to rely on numerical simulations and analytical studies to aid our understanding on this problem. As the beginning of this challenging task, we start with this problem of a two-dimensional rarefied gas jet impingement on a flat plate surface.

This paper is organized as follows: Section II describes the problem, and provides some analysis and corresponding exact solutions; Section III provides some validations by comparing the analytical results with some particle simulation results; and Section IV summarizes this study.

II. Two-dimensional Rarefied Jet Impinging on a Flat Plate

This section discusses the problem of a rarefied two-dimensional jet impinging on a flat plate, especially we concentrate on the case of collisionless flow situation. Besides the macroscopic flowfield properties, we are specifically interested in the slip velocity, pressure and shear stress on the plate surface. Based on these analytical results, we can provide estimations for less rarefied flow situations in the range of Knudsen number larger than 1.0.

Figure 1 illustrates the problem. Rarefied plume jet, with known number density n_0, average velocity U_0, and temperature T_0, is fired from a nozzle of a width D. One plate is placed at a distance of L to the nozzle, and the plate semi-height is W. The plate may extend widly or even to infinity for specific applications. In this situation, the contribution to any macroscopic properties consists of two parts: the free plume flow from the left nozzle, and the collective effects of reflections from the right plate. As such, the velocity phase for point $P(X,Y)$ consists of two parts, one part is from the nozzle, shown at the left side of Fig.2; and the other by the plate, shown as the right side of Fig.2.

A. Solutions For Two-dimensional Free Molecular Jet Plume Expanding Into Vacuum

Before we proceed to solve the problem of a jet plume impinging on a flat plate, first we need to review the detailed flow field solutions for a two-dimensional collisionless jet flow expanding into vacuum. This is because it is the foundation for the impingement problem.

In one previous study,[9] a general relation between geometry relation and velocity directions was followed. If the slit semi-height is $H = D/2$ and we consider the velocity space for a point (X,Y) in front of the slit, the velocity distribution at the point follows the Maxwellian distribution, the integral domain does not necessarily include the origin because of the non-zero average exit velocity. From any point $(0,y)$ on the nozzle exit, particles can arrive at the point (X,Y) if and only if their velocity components satisfy the following relation:

$$\tan\theta = \frac{Y-y}{X} = \frac{v}{u+U_0}, -H < y < H. \tag{1}$$

The velocity phase domain starts with a value of (-U_0, 0). Hence, $u+U_0$ represents a particle's actual velocity along the X-direction. Obviously the non-zero average velocity U_0 does not destroy the one-to-one mapping relation between the two velocity phase spaces, the distribution is still Maxwellian. It uniquely maps the velocity distribution domain for the point $(0,y)$ at the nozzle exit to the point (X,Y). The velocity phase is shown as the shaded region in the left part in Fig.2.

$$\tan\theta_2 = \frac{Y+H}{X}, \tan\theta_1 = \frac{Y-H}{X} \tag{2}$$

where $\theta_2 > \theta_1$, $0 < \theta_2 < \pi/2$ and $-\pi/2 < \theta_1 < \pi/2$, for the free plume problem, we can derive the number density, velocities and temperature at any point (X,Y) in front of the slit:[9]

$$\frac{n_1(X,Y)}{n_0} = \frac{\exp(-S_0^2)}{2\pi}(\theta_2-\theta_1) + \frac{1}{4}\Big(\mathrm{erf}(S_0\sin\theta_2) - \mathrm{erf}(S_0\sin\theta_1)\Big) + \frac{S_0}{2\sqrt{\pi}}\gamma_0(\theta_1,\theta_2) \tag{3}$$

$$\frac{U_1(X,Y)}{\sqrt{2RT_0}} = \frac{\exp(-S_0^2)}{2\pi}\frac{n_0}{n_1}\left[\frac{\sqrt{\pi}}{2}\gamma_1(\theta_1,\theta_2) + \frac{S_0(\theta_2-\theta_1)}{2} + \frac{S_0(\sin(2\theta_2)-\sin(2\theta_1))}{4} + S_0^2\sqrt{\pi}\gamma_2(\theta_1,\theta_2)\right] \tag{4}$$

$$\frac{V_1(X,Y)}{\sqrt{2RT_0}} = \frac{1}{4\sqrt{\pi}}\frac{n_0}{n_1}\Big[\gamma_3(\theta_1) - \gamma_3(\theta_2)\Big] \tag{5}$$

where the subscript '$_1$' represents the free plume expansion solutions and $S_0 = U_0/\sqrt{2RT_0}$ represents the plume exiting speed ratio. More details and validation work about n_1, U_1, and V_1 solutions are available in the previous study,[9] for convenience to the readers, we solely present the results here. Further, the temperature field solution is:

$$\frac{T_1(X,Y)}{T_0} = -\frac{U_1^2+V_1^2}{3RT_0} + \frac{\exp(-S_0^2)}{6\pi}\frac{n_0}{n_1}\left[(3+S_0^2)\Delta\theta + \frac{S_0^2}{2}[\sin(2\theta_2)-\sin(2\theta_1)] + 2S_0\sqrt{\pi}(2\gamma_1+S_0^2\gamma_2)\right] \tag{6}$$

where:

$$\gamma_0(\theta_1,\theta_2) = \int_{\theta_1}^{\theta_2}\exp(-S_0^2\sin^2\theta)\cos\theta\,\mathrm{erf}(S_0\cos\theta)d\theta \tag{7}$$

$$\gamma_1(\theta_1,\theta_2) = \int_{\theta_1}^{\theta_2} \exp(S_0^2\cos^2\theta)\cos\theta[1+\mathrm{erf}(S_0\cos\theta)]d\theta \tag{8}$$

$$\gamma_2(\theta_1,\theta_2) = \int_{\theta_1}^{\theta_2} \exp(S_0^2\cos^2\theta)\cos^3\theta[1+\mathrm{erf}(S_0\cos\theta)]d\theta \tag{9}$$

$$\gamma_3(\theta) = \exp(-S_0^2\sin^2\theta)\cos\theta[1+\mathrm{erf}(S_0\cos\theta)] \tag{10}$$

The pressure expression is available from the equation of state, with known $n_1(X,Y)$ and $T_1(X,Y)$. It is evident that this set of solutions includes two types of factors: geometry factors, θ_1, θ_2 and the plume exiting speed ratio, S_0.

Because the flows are rarefied, it is appropriate to utilize the direct simulation Monte Carlo (DSMC) method,[17] to validate the analytical results. For the validation work, we use argon gas, and a simple square simulation domain, and the collision function is turned off to achieve the collisionless effects. For this situation, the value of the number density at the exit does not produce any difference in the final normalized results and exact free molecular flows are guaranteed.

Figure (3) shows pressure contours for a free plume flow (without plate), evaluated with the analytical and simulation methods. The comparison shows virtually identical results. Because the pressure results involve n_1, U_1, V_1 and T_1, the perfect agreement between the DSMC and the analytical results prove that all other analytical expressions are valid as well.

B. Collisionless Plume Impingement Problem: Vertical Plate Properties

The number density on the plate consists of two terms:

$$n_2(L,y) = n_1(L,y) + n'_w(y) \tag{11}$$

where the left hand side term $n_2(L,y)$ is the density solution for the plume impingement problem. At the right hand side, $n'_w(y)$ is the new density factor contributed from the plate, and $n_1(L,y)$ is the free plume solution directly evaluated from Eqn.(3).

The derivation of $n'_w(y)$ is presented in another paper.[19] It is evident that the velocity $U_2(L,y)$ is zero along the plate surface due to the non-penetration condition, and we utilize this condition to determine $n'_w(y)$. Suppose the velocity distribution function for those reflected particles is:

$$f_w(y) = n_w(y)(\beta_w/\pi)\exp[-\beta_w(u^2+v^2)] \tag{12}$$

Then from an integration with u as the moment, we obtain:

$$n_1(L,y)U_1(L,y) = -\int_{-\infty}^{\infty}\int_{-\infty}^{0} u f_w(y)dudv = \frac{n_w\sqrt{T_w R}}{\sqrt{2\pi}} \tag{13}$$

where "$_1$" represents the free plume flow properties in the flowfield without any plate effects. By integrating Eqn.(12) with the left half of the velocity space, we obtain the contributions from the plate to $n_2(L,y)$:

$$n'_w(y) = \sqrt{\frac{\pi}{2}}\frac{n_1(L,y)U_1(L,y)}{\sqrt{RT_w}} \tag{14}$$

The number density cannot be directly sampled as a plate property in the DSMC simulation, it shall be extracted from locations in the flowfield adjacent to the plate.

The slip velocity at the plate is obtained with the following relation:

$$V_2(L,y) = n_1(L,y)V_1(L,y)/n_2(L,y) = \frac{V_1}{1+\sqrt{\pi\beta_w}U_1} \tag{15}$$

The contribution to the slip velocity from the plate velocity distribution, Eqn.(12), is zero because we assume the plate is completely diffuse. With the symmetric velocity phase about the X-axis, the contributions from the plate to the above equation is zero. This slip-velocity is important for simulations of the interactions between dust particle and gas with the Discrete Element Method (DEM),[20,21] because it provides the crucial input data.

The temperature and pressure at locations close to the plate, i.e., at a flowfield point, are:

$$T_2(L-,y)/T_0 \quad = -\frac{V_2^2}{3RT_0} + \frac{n_w}{2n_2\epsilon} + \frac{n_1}{n_2}\left(\frac{T_1}{T_0} + \frac{U_1^2+V_1^2}{3RT_0}\right) \tag{16}$$

$$P_2(L-,y) = n_2(L,y)kT(L-,y) \tag{17}$$

where $\epsilon = T_0/T_w$. No matter how close to the plate a point locates, the temperature and pressure definitions for the point are averaged properties along the x-, y- and z- directions. The temperature is important to evaluate the viscosity at locations close to the plate, and it is a required input parameter for a DEM simulation as well.

Since the plate normal direction is defined as $(-1,0)$ at the plate surface, we can obtain other properties such as pressure, and shear stress on the plate, with simpler formats:

$$T_2(L,y)/T_0 \quad = \frac{n_w}{2n_2\epsilon} + \frac{\exp(-S_0^2)}{2\pi}\frac{n_0}{n_2}\left[(2+S_0^2)\Delta\theta + \frac{S_0^2}{2}(\sin 2\theta_2 - \sin 2\theta_1) + S_0\sqrt{\pi}(3\gamma_1 + 2S_0^2\gamma_2)\right] \tag{18}$$

$$C_f = \frac{\tau_{xy}}{\rho U_0^2/2} \quad = \frac{1}{2\pi S_0^2}\left[(\cos^2\theta_1 - \cos^2\theta_2)\exp(-S_0^2) + S_0\sqrt{\pi}[\cos^2\theta_1\gamma_3(\theta_1) - \cos^2\theta_2\gamma_3(\theta_2)]\right] \tag{19}$$

For some engineering applications, the location with the maximum shear stress is of special interest, for example, the lunar ground breaks off firstly there. We can obtain such a location from the Eqn.(19) implicitly for a two-dimensional case. With some assumptions, we obtain the following simple formula for the critical location with the maximum shear stress:

$$\frac{y_{crit}}{D} = \sqrt{\frac{(L/D)^2}{3S_0^2} - \frac{1}{12}} \approx \frac{1}{\sqrt{3}S_0}\frac{L}{D} \tag{20}$$

The above approximation is based on assumptions that L/D is large and the exit speed ratio is not large. In one NASA's dust experiment, it is found the largest ground shear stress happens at a location proportional to L/D, while inversely proportionably to the nozzle exit Mach number.[22] As such, the above equation provides a strong support for the highly rarefied gas flow situation. With the simple result for the location with the largest shear stress, the simplified maximum shear stress value is:

$$C_{f,max} = \frac{\tau_{max}}{\rho_0 U_0^2/2} = \frac{1}{2\sqrt{3\pi}}[1+\mathrm{erf}(S_0)][1+\frac{3}{2S_0^2}]\frac{D}{L} \tag{21}$$

From the above equation, we can obtain the following bounding limits for the normalized shear stress:

$$\frac{1}{2\sqrt{3\pi}}\frac{D}{L} \le \frac{1}{2\sqrt{3\pi}}[\frac{3}{2S_0^2}+1]\frac{D}{L} \le \frac{\tau_{max}}{\rho_0 U_0^2/2} \le \frac{1}{\sqrt{3\pi}}[\frac{3}{2S_0^2}+1]\frac{D}{L} \tag{22}$$

The above two equations are simple and they reflect that: 1) the critical position is almost linearly related with L/D, and inversely proportional to the exit speed ratio S_0; 2) the normalized maximum shear stress is inversely proportional to L/D. For rocket plume interactions with the lunar ground, usually the ground breaks at the locations with the highest shear stress, according to the Roberts' model,[23] the deepest crater location is not at the plume centerline. With this critical point determined we can conveniently determine the shear stress curve for any collisionless flow.

The heat flux on the plate surface has the following final analytical format:

$$\begin{aligned}\frac{q}{\rho U_0^3/2} \quad &= \frac{\exp(-S_0^2)}{4\pi S_0^3}\Big[(2+\beta_0 V_2^2)\sqrt{\pi}\gamma_1 + (7+2\beta_0 V_2^2)\sqrt{\pi}S_0^2\gamma_2 + 2S_0^4\sqrt{\pi}\gamma_4 + \\ &\int_{\theta_1}^{\theta_2}\Big((6+2\beta_0 V_2^2)S_0\cos^2\theta + 2S_0^3\cos^4\theta\Big)d\theta\Big] - \\ &\frac{V_2\sqrt{\beta_0}}{2\pi S_0^3}\int_{\theta_1}^{\theta_2}\sin\theta\Big(S_0\sqrt{\pi}\gamma_3(\theta)[2S_0^2\cos^2\theta+3] + 2\cos\theta + 2S_0^2\cos^3\theta\Big)d\theta - \frac{1}{S_0^3\sqrt{\pi\epsilon^3}}\frac{n_w}{n_0}\left[1+\frac{\beta_w}{2}V_2^2\right]\end{aligned} \tag{23}$$

where

$$\gamma_4(\theta_1,\theta_2) = \int_{\theta_1}^{\theta_2}\exp(S_0^2\cos^2\theta)\cos^5\theta[1+\mathrm{erf}(S_0\cos\theta)]d\theta \tag{24}$$

C. Flowfield Solutions

Finally, we provide some flowfield solutions as follows. The density field $n_2(X,Y)$ in front of the plate is:

$$n_2(X,Y) = n_1(X,Y) + \frac{1}{2\pi}\int_{\phi_1}^{\phi_2} n_w(\phi)d\phi = n_1(X,Y) + \frac{L-X}{2\pi}\int_{W}^{-W} \frac{n_w(y_0)}{(Y-y_0)^2+(X-L)^2}dy_0 \tag{25}$$

where the integral part is the contribution from the plate, with ϕ as the slope of a line connecting point $P(X,Y)$ and a specific point (L,y_0) on the plate. The integration on ϕ is changed to an integration over y_0, with the following relation:

$$\frac{u}{v} = \tan(\phi) = \frac{X-L}{Y-y_0} \tag{26}$$

and

$$d\phi = \frac{L-X}{(Y-y_0)^2+(X-L)^2}dy_0 \tag{27}$$

The integration on y_0 ranges from finite value $(-W,W)$, which is applicable for certain applications. For applications such as rocket plume-lunar ground interactions, we can extend W to ∞. The flowfield velocity solutions are as follows:

$$U_2(X,Y) = \left(n_1(X,Y)U_1(X,Y) + \frac{(L-X)^2}{2\pi}\int_{W}^{-W} \frac{n_w(y_0)}{(Y-y_0)^3+(X-L)^3}dy_0\right)/n_2(X,Y) \tag{28}$$

$$V_2(X,Y) = \left(n_1(X,Y)V_1(X,Y) + \frac{(L-X)}{2\pi}\int_{W}^{-W} \frac{n_w(y_0)(Y-y_0)}{(Y-y_0)^3+(X-L)^3}dy_0\right)/n_2(X,Y) \tag{29}$$

At the end of this section, we want to point it out that for flowfield evaluations via a computer, Eqns.(25, 28, 29) are the most convenient formats. For other purposes which require more concise analytical formats, it is possible to provide some further simplifications.

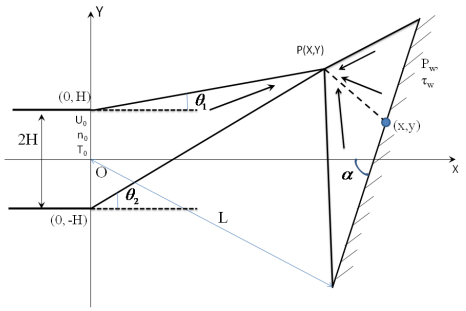

Figure 1. Illustration for the plume impingement problem, the right side is an inclined plate.

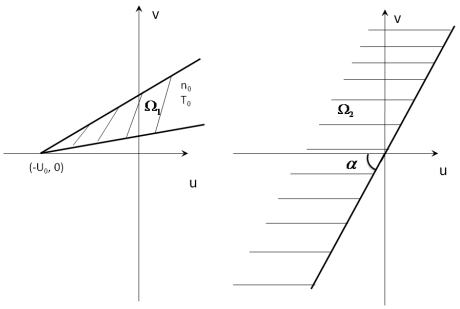

Figure 2. Velocity phases for a point on the the inclined surface.

III. Validations

In this section, we validate the above analytical results with a specific particle simulation package named GRASP,[18] which is developed at New Mexico State University. First we validate the collisionless flow solutions; further we extend the results to finite Knudsen number case with Kn=1. We simulate a collisionless jet impinging on a plate with $S_0 = 2$. The gas is Argon, the nozzle diameter is $D = 0.2$ m, and the nozzle height $L = 2.0$ m. The collision function in the DSMC package is switched off, as such, the $Kn = \infty$ condition is achieved. Figure 4 shows the normalized density for the case of $Kn = \infty$ with $S_0 = 2$. The analytical and the DSMC simulation results have almost identical agreement, due to the blockage effects from the plate, at locations close to the plate the density values are relative high. Compared with the free jet problem, in the top regions, the density contours completely change; however, the analytical results successfully capture the distributions. Figure 5 shows the normalized U-velocity distribution contours for the flowfield with a

vertical flat plate, $S_0 = 2$ and $Kn = \infty$. In this figure, the U-Velocity at the plate surface is zero due to the non-penetration condition. Along the plume centerline, the velocity decreases when the x-coordinate increases. Figure 6 shows the normalized V-velocity contours for this benchmark case, the contours have much complex patterns than the U-velocity contours, the V-velocity expands much faster than the U-velocity when the Y-coordinates increase.

For the near plate or on plate properties, we are specially concerned with the slip-velocity, pressure, shear stress and heat flux distributions along the plate because of two reasons. First, for most plume impingement applications, the pressure and shear stress distributions are important. For DEM simulation of lunar dust flow, the ground slip velocity distribution is another necessary input variable. Secondly, the agreement of pressure distribution can support well the validity of the number density and temperature results. In fact, we confirm that the agreement between the analytical results and the simulation results of density and temperature are perfect.

Figure 7 shows the slip velocity profiles along the plate for the case of collisionless flows. The DSMC simulation results are extracted from locations close to the plate. Figure 8 shows the pressure on the plate surface, since the plate normal direction is determined, the pressure for this situation merely includes the component related to the normal direction. The analytical treatment and the DSMC simulation have consistent results. It is evident that the pressure value on the plate is much larger than the near plate flowfield averaged values. This is due to the fact that the major flow velocity direction change happens along the X-direction, as such, the velocity distribution function along the X-direction is much wider than the other two directions. The analytical results have almost identical results with those simulation results. Figures 9 and 10 show the plate shear stress and heat flux respectively for $Kn = \infty$ with different S_0, the analytical and the DSMC simulation results are virtually identical.

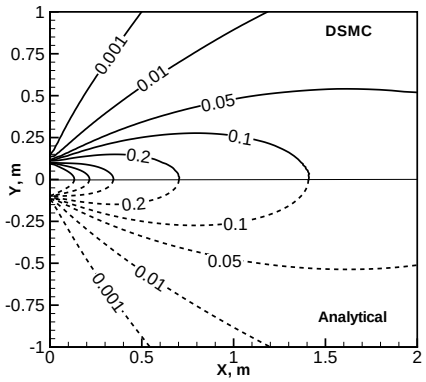

Figure 3. Comparison of normalized pressure distribution of the free plume, $S_0 = 1$, free molecular, H=0.1 m. Top: DSMC, Bottom: Analytical.

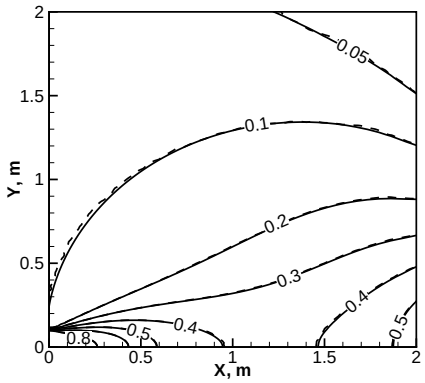

Figure 4. Contours of normalized density for the vertical plate case, $Kn = \infty$, $S_0 = 2$, $H = 0.1$ m, $L = 2.0$ m, left bottom corner: nozzle, right border: plate.

IV. Summary

We have analyzed the problem of rarefied two-dimensional jet flows impinging on a flat plate, and validated the results. First we present the complete solutions for free molecular plume flow expanding into vacuum. By adopting a velocity-direction and geometry relation, we have successfully obtained the flowfield density, velocity, temperature and pressure distributions. These results are helpful to study less rarefied free plume flows and are the foundations for the plume impingement problem. By adding an extra plate, we derived some properties close to the plate and the on-plate shear stress, pressure distributions, slip velocities, and some flowfield properties. For collisionless flows, the analytical results are virtually identical to the DSMC simulations results.

For the large range of rarefied regimes with $Kn \geq 1$, we can adopt the analytical results presented in this paper for fast engineering estimations with minor discrepancies. Even though the analytical results are complex, the evaluation speed is much faster than the DSMC simulations; the detailed exact analytical

results permit us to study different factors systematically. One example is the critical location on the plate with the largest shear stress, which is critical for the problem of rocket plume and lunar ground interactions.

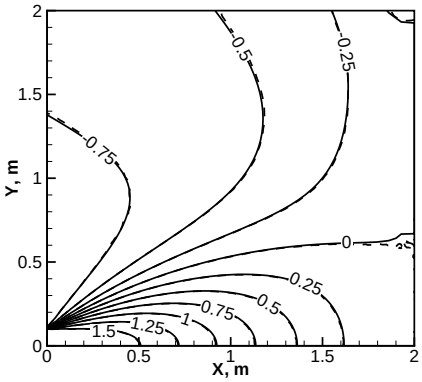

Figure 5. Contours of normalized U-velocity for the vertical plate case, $Kn = \infty$, $S_0 = 2$, $H = 0.1$ m, $L = 2.0$ m, left bottom corner: nozzle, right border: plate.

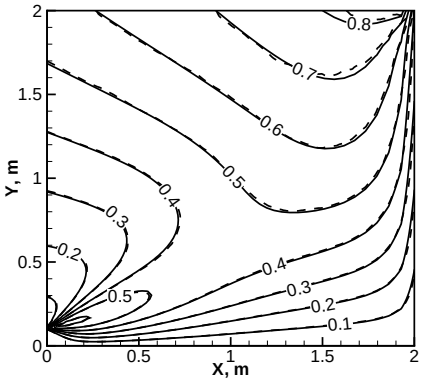

Figure 6. Contours of normalized V-velocity for the vertical plate case, $Kn = \infty$, $S_0 = 2$, $H = 0.1$ m, $L = 2.0$ m, left bottom corner: nozzle, right border: plate.

Acknowledgement

We gratefully acknowledge the support from the National Science Foundation grant CBET-0854411.

References

[1]Maev, R. and Leshchynsky, V., *Introduciton to Low Pressure Gas Dynamic Spray*, Wiley-Vch, Weinheim, Germany, 2008.

[2]Hastings, D. and Garrett, H., *Spacecraft-Environment Interactions*, Cambridge Univ. Press, Cambridage, UK., 1996.

[3]Woronowicz, M. S., "On Plume Flowfield Analysis and Simulation Techniques," AIAA paper 1994-2048, the 6th AIAA/ASME Joint Thermophysics and Heat Transfer Conference, June 20-23, 1994, Colorado Springs, CO.

[4]Liepmann, H. W., "Gas kinetics and Gasdynamics of Orifice Flow," *Journal of Fluid Mechanics*, Vol. 10, No.1., 1961, pp. 65-79.

[5]Narasimha, R., "Orifice Flow of High Knudsen Number," *Journal of Fluid Mechanics*, Vol. 10, No. 3, 1961, pp. 371-384.

[6]Brook, J. W., "Density Field of Directed Free-Molecular Flow From An Annulus," *Journal of Spacecraft*, Vol. 6, No. 6, 1969, pp. 755-757.

[7]Lilly, T. C., Gimelshein, S.F., Ketsdever, A.D. and Markelov, G.N., "Measurements and Computations of Mass Flow and Momentum Flux Througth Short Tubes in Rarefied Gases," *Physics of Fluids*, Vol. 18, No. 9, 2006.

[8]Narasimha, R., "Collisionless Expansion of Gases Into Vacuum," *Journal of Fluid Mechanics*, Vol. 12, No. 3, 1962, pp. 294-308.

[9]Cai, C. and Boyd, I. D., "Theoretical and Numerical Study of Several Free Molecular Flow Problems," *Journal of Spacecraft and Rocket*, Vol. 44, No. 3, May-June, 2007, pp. 619-624.

[10]Cai, C. and Boyd, I. D., "Collisionless Gas Flow Expanding into Vacuum", *J. Spacecraft and Rockets*, Vol. 44, No. 6, November-December, 2007, pp. 1326-1330.

[11]Weaver, D. P., Wysong, I., Ketsdever, A., Campbell, D., Vaghijiani, G., Wadsworth, D. and Alfano, A., April, 2005, AFRL-PR-ED-TR-2005-0035.

[12]Bradshaw, B. A., and Love, E. M., "The Normal Impingment of a Circular Air Jet On a Flat Surface," Aeronautical Research Council Reports and Memoranda, No. 3205, Bedford, September, 1959.

[13]Sathian, S. P. and Kurian, J., "Studies on Impingment Effects of Low Density Jetson Surfaces-Determination of Shear Stress and Normal Pressure," International Symposium on Rarefied Gas Dynamics, Monopoli(Bari), Italy, July-10-16, 2004.

[14]Maddox, A.R., "Impingment of Under Expanded Plumes on Adjacent Surfaces," *J. Spacecraft*, Vol. 5, No. 6, 1968, pp. 718-724.

[15]Kannenberg, K. and Boyd, I., "Three-Dimensional Monte Carlo Simulations of Plume Impingement," *J. Thermophysics and Heat Transfer*, Vol. 13, No. 2, 1999, pp. 226-235.

[16]Metzger, P. T. and Immer, C. D., "Jet-Induced Cratering of a Grannular Surface With Application to Lunar Spaceports," *Journal of Aerospace Engineering*, Vol. 22, No. 1, 2009, pp. 24-32.

[17]Bird, G. A., *Molecular Gas Dynamics and the Direct Simulation of Gas Flows,* Oxford Univ. Press, New York, 1994.

[18]Liu, H and Cai, C., "An Object-Oriented Serial DSMC Simulation Package," 27th International Rarefied Gasdynamics Symposium, Pacific Grove, CA, July 10-15, 2010.

[19]Khasawneh, K., Liu, H. and Cai, C. "Highly Rarefied Two-Dimensional Jet Impingement on a Flat Plate," *Physics of Fluids*, Vol. 22, No. 11, 2010, pp. 117101-117106.

[20]Gethin, D., Yang, X. and Lewis, R., "A Two Dimensional Combined Discrete and Finite Element Scheme for Simulating the Flow and Compaction of Systems Comprising Irregular Particulates," *Computer Methods in Applied Mechanics and Engineering,* 195, 2006, pp. 5552-5565

[21]Munjiza, A., *The Combined Finite-Discrete Element Method,* John Wiley and Son, Cichester, 2004.

[22]Clark, L. V. and Land N. S., "Experimental Investigation of Jet Impingement on Surfaces of Fine Particles in a Vacuum Environment," NASA-TN-D-2633,1965

[23]Roberts, L., "The Action of A Hypersonic Jet On a Dust Layer," IAS Paper, No.63-50, Institute of Aerospace Sciences 31st Annual Meeting, New York.

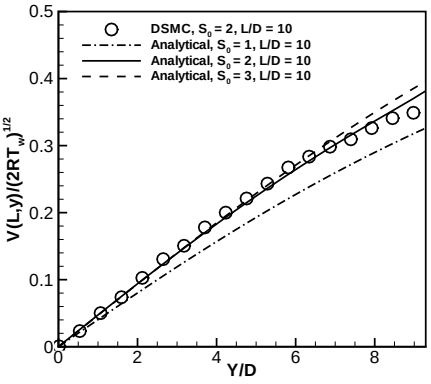

Figure 7. Profiles of normalized slip velocity for the vertical plate case, $V(L,y)/\sqrt{2RT_w}$, collisionless.

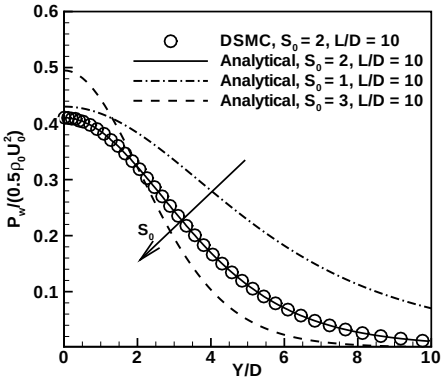

Figure 8. Profiles of normalized pressure on the plate for the vertical plate case, $P(L,y)/(\rho_0 U_0^2/2)$, collisionless, $L/D = 10$.

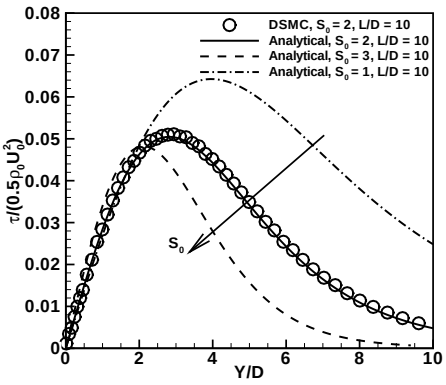

%hfill

Figure 9. Profiles of normalized shear stress on the plate for the vertical plate case, $\tau_{xy}/(\rho_0 U_0^2/2)$, collisionless, $L/D = 10$.

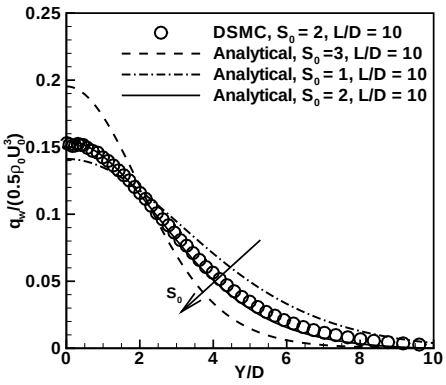

Figure 10. Profiles of normalized heat flux on the plate for the vertical plate case, $q_w/(\rho_0 U_0^3/2)$, collisionless, $L/D = 10$.